New Journal of Physics
The open access journal at the forefront of physics

Deutsche Physikalische Gesellschaft DPG IOP Institute of Physics

PAPER • OPEN ACCESS

Non-Fermi-liquid to Fermi-liquid transports in iron-pnictide $Ba(Fe_{1-x}Co_x)_2As_2$ and the electronic correlation strength in superconductors newly probed by the normal-state Hall angle

To cite this article: L M Wang *et al* 2017 *New J. Phys.* **19** 033039

New Journal of Physics
The open access journal at the forefront of physics

Deutsche Physikalische Gesellschaft DPG
IOP Institute of Physics

Published in partnership with: Deutsche Physikalische Gesellschaft and the Institute of Physics

OPEN ACCESS

RECEIVED
11 December 2016

REVISED
10 February 2017

ACCEPTED FOR PUBLICATION
6 March 2017

PUBLISHED
28 March 2017

PAPER

Non-Fermi-liquid to Fermi-liquid transports in iron-pnictide $Ba(Fe_{1-x}Co_x)_2As_2$ and the electronic correlation strength in superconductors newly probed by the normal-state Hall angle

L M Wang[1], Chih-Yi Wang[1], Sha-Min Zen[1], Jin-Yuan Chang[1], C N Kuo[2], C S Lue[2], L J Chang[2], Y Su[3], Th Wolf[4] and P Adelmann[4]

[1] Graduate Institute of Applied Physics/Department of Physics, National Taiwan University, Taipei 106, Taiwan
[2] Department of Physics, National Cheng Kung University, Tainan 70101, Taiwan
[3] Jülich Centre for Neutron Science (JCNS), Institut für Festk rperforschung, Forschungszentrum Jülich, Outstation at FRM-II, Lichtenbergstrasse 1, D-85747 Garching, Germany
[4] Karlsruhe Institute of Technology (KIT), Institut fuer Festkoerperphysik, D-76021, Karlsruhe, Germany

E-mail: liminwang@ntu.edu.tw

Keywords: iron-based superconductor, electronic correlation, non-Fermi-liquid, Hall angle

Abstract

Electrical transports in iron-pnictide $Ba(Fe_{1-x}Co_x)_2As_2$ (BFCA) single crystals are heavily debated in terms of the hidden Fermi-liquid (HFL) and holographic theories. Both HFL and holographic theories provide consistent physic pictures and propose a universal expression of resistivity to describe the crossover of transports from the non-Fermi-liquid (FL) to FL behavior in these so-called 'strange metal' systems. The deduced spin exchange energy J and model-dependent energy scale W in BFCA are almost the same, or are of the same order of several hundred Kelvin for over-doped BFCA, which is in agreement with the HFL theory. Moreover, a drawn line of $W/3.5$ for BFCA in the higher-doping region up to the right demonstrates the crossover from non-FL-like behavior to FL-like behavior at high doping, and shows a new phase diagram of BFCA. The electronic correlation strength in superconductors has been newly probed by the normal-state Hall angle, which found that, for the first time, correlation strength can be characterized by the ratios of T_c to the Fermi temperature T_F, J/T_F, and the transverse mass to longitudinal mass.

1. Introduction

The 'strange-metal' transports in high-temperature superconducting (HTS) cuprates, as well as in new iron-based superconductors, have been the subject of intense study. In particular, the amazing similarity between the quantum-mechanical phase diagrams of cuprates and iron-based superconductors reveals that both of their superconductivities are ascribed to the quantum critical fluctuations associated with a quantum critical point (QCP), even though HTS cuprates are doped Mott insulators, while iron-based superconductors are metallic systems [1, 2]. Within the quantum-mechanical phase transition, the singular QCP at absolute zero produces a wide region of unusual behavior at a finite temperature, which displays a striking deviation from the conventional Fermi-liquid (FL) behavior, as it has the so-called strange-metal transport properties [3]. Understanding this QCP is essential, as it corresponds to the occurrence of superconductivity in the vicinity of spin-density-wave (SDW) instability or antiferromagnetic fluctuation [1, 4]. Recently, a number of experiments on iron-based superconductors showed a phase transition involving the onset of a SDW order in the normal state above T_c, which extrapolates to a $T = 0$ SDW QCP (see [5] and the references therein). For example, the SDW transition was observed in both the resistivity and susceptibility of $BaFe_{2-x}Co_xAs_2$ single crystals in the underdoped region [6]. A more recent study on electronic specific heat in $BaFe_{2-x}Ni_xAs_2$ indicates that the effect of spin fluctuation should not be ignored [7]. It even has been proposed that, SDW QCP is a central organizing principle of organic, iron-pnictide, heavy-fermion, and HTS cuprates [8–10]. Under QCP (i.e. optimum doping), the strongest magnetic spin fluctuation suppresses the SDW order, accompanies the appearance of the

highest T_c, and results in non-FL-like scattering associated with Fermi-surface reconstruction. Electrical resistivity measurements reveal a remarkably T-linear behavior for samples near the optimum doping, while a T^2-dependent feature can be observed in the higher-doping region [11].

In the phase diagram, a line is usually drawn up and to the right from the edge of the superconducting dome in the higher-doping region in order to separate the non-FL (NFL) 'strange metal' from a conventional Fermi liquid (FL) at high doping [12]. In addition to dc resistivity, measurements of optical conductivity show a T-linear scattering characteristic for samples near the optimum doping, which can be ascribed to a two-dimensional (2D) metal at the onset of the SDW order [13, 14]. Particularly, recent studies of infrared spectra, interplane resistivity, and transport coefficients on iron-based superconductors reveal a possible pseudogap in the phase diagrams, which are similar to those observed in HTS cuprates [15–17]. These phenomena remain a major open question in the physics of strongly correlated electrons.

Recently, the hidden FL (HFL) theory [18, 19] and holographic models [20] have been respectively developed to express the transport and spectroscopic properties of over-doped HTS cuprates for the entire normal state. Based on theoretical studies, it is argued that there is no clear transition line to a true FL for higher doping in the phase diagram. Self-consistency of HFL has been shown in the transport and spectroscopic properties of $Tl_2Ba_2CuO_y$ and $La_{2-x}Sr_xCuO_4$ systems [18, 19]; however, the availabilities of HFL and holography have never been examined in iron-based superconductors. Theoretical works have been further developed and cast into the framework of strongly correlated FLs or quantum critical systems [20, 21]. Recent optical studies on $BaFe_{2-x}Ni_xAs_2$ and $Ba_{0.6}K_{0.4}Fe_2As_2$ single crystals further show the interesting hidden-T-dependent properties of the two Drude models, and have proposed the hidden NFL behavior in the underdoped samples [2, 13]. In particular, the boundary from NFL T dependence to FL T^2 dependence, as observed in resistivity measurements, is not clear for iron-based pnictides [22, 23]; whereas, the boundary can be obtained by the departure of resistivity from linearity for over-doped cuprates [24].

This article debates and discusses the resistivities and Hall angles of $Ba(Fe_{1-x}Co_x)As_2$ (BFCA) single crystals in terms of the existing theories. It is found herein that the deduced bandwidth of the spin excitation (the spin exchange energy J) from the Hall angle is in agreement with bandwidth W, as determined from resistivity by considering the HFL theory. An additional phase boundary line corresponding to the crossover from NFL-like transport to FL-like transport can be obtained in the new phase diagram of BFCA. Furthermore, the spin exchange energies for some conventional and unconventional superconductors, as derived from Hall measurements, are developed to explore their electronic correlation strength. The ratios of the spin exchange energy to Fermi temperature T_F, J/T_F, as well as the transverse mass to longitudinal mass, are presented for the first time in order to characterize the electronic correlation strength in superconductors.

2. Theoretical surveys

Previous theoretical attempts to explain the crossover from NFL to FL in the transport properties of HTS cuprates are based on the assumption that, transport lifetime, τ_{tr}, must include two different scattering lifetimes, which independently influence the temperature dependence of longitudinal resistivity ρ_{xx}. In the HFL theory, resistivity is explained in terms of the bottleneck effect, where there are two different dissipative processes for accelerated electrons, umklapp scattering and quasiparticle decaying into one pseudoparticle. These two processes act in series to dissipate the momentum to the lattice [18]. However, in holographic models [20], the electrical transport is described by two contributions to conductivity, a charge-conjugation symmetric term and another from explicit charge density relaxed by some momentum dissipation. Although arising from completely different models, both theories provide a consistent picture, which consider the T^2-dependent relaxation rate and linear-T decay process in pseudoparticle conductivity, in order to achieve a universal expression of resistivity:

$$\rho_{xx} = A\frac{T^2}{T+W} + \rho_0, \tag{1}$$

where A is a temperature-independent pre-factor, W is a model-dependent energy scale, and ρ_0 is the residual resistivity. For $T \gg W$, one can see that $\rho_{xx} \approx AT + \rho_0$; while $\rho_{xx} \approx \Lambda T^2 + \rho_0$ with $\Lambda = A/W$ for $T \ll W$. In the HFL theory, pre-factor A corresponds to $\frac{\hbar}{e^2}\frac{1}{E_F}\left(\frac{v_{F0}}{v_F}\right)$, and Λ is equal to $\frac{\hbar}{e^2}\frac{1}{E_F}\left(\frac{1}{W}\right)$, where v_{F0} is the maximum Fermi velocity, E_F is the Fermi energy in unit of temperature, and W corresponds to the bandwidth of the spin excitations for 2D resistivity [18]. Let us now look at the W value in detail from the new light of the holographic theory, where W can be represented by $W = A/\Lambda$. Ito *et al* [25] considered that $\rho_{xx} = (4\pi/\omega_{pD}^2)\tau^{-1}$ with scattering rate $\hbar\tau^{-1} = \lambda T$, the Drude spectral weight is $\omega_{pD}^2 \approx n_{eff}/m^*$ (n_{eff} and m^*, which are effective carrier density and effective mass, respectively), and λ (≈ 0.3) is the coupling strength between the charge carriers and spin excitations in the HTS cuprates. Considering $m^* = (\hbar^2/E_F)\pi n_{eff}$ for a 2D system, the pre-factor A in T-linear resistivity can be estimated to be $\frac{\hbar}{e^2}\frac{1}{E_F}4\pi^2\lambda$, which is similar to that presented in the HFL theory. On the

other hand, the electron–electron scattering processes are given by $\hbar/\tau_{e-e} = A^*T^2/E_F$, where A^* is a dimensionless constant with $A^* \approx 4$ for BFCA [1], resulting in electron–electron-scattering resistivity ρ_{e-e}, where $\rho_{e-e} = m^*/(n_{eff}\, e^2\, \tau_{e-e}) = \frac{\hbar}{e^2}\left(\frac{1}{E_F}\right)^2 \pi A^* T^2$, and $\Lambda = \frac{\hbar}{e^2}\left(\frac{1}{E_F}\right)^2 \pi A^*$. Thus we have $W = A/\Lambda = (4\pi/A^*)\, E_F\lambda$, indicating that W is related to the Fermi energy and coupling strength when the holographic theory is considered. Although model-dependent energy scale W represents different meanings in the physics of the HFL and holography theories, in both theories it characterizes the crossover from NFL to FL, and can reflect the electrical coupling strength in the normal-state transports of superconducting systems, as seen later in the discussions of temperature-dependent resistivity and Hall angle.

Anderson and Casey [18] fitted equation (1) to the resistivity data of $La_{2-x}Sr_xCuO_4$, with x ranging from underdoping of $x = 0.15$ to overdoping of $x = 0.33$; and obtained the doping-dependent W, which is in the order of a few hundred kelvins and in agreement with those determined from Hall and angle-resolved photoemission spectroscopy analysis. A similar result of overdoped HTS $Tl_2Ba_2CuO_{6+\delta}$ with $W = 800$ K was obtained by Casey and Anderson [19].

Theoretical attempts on explaining the anomalous transport properties of HTS cuprates, where resistivity and the Hall effect have different temperature dependencies, are based on the assumption that there exists two transport relaxation times, which independently influence the Hall effect and resistivity in these systems. An important advance in explaining this anomalous behavior in the cuprates was Anderson's conjecture that there exist two transport relaxation times in the cuprates that independently influence the Hall effect and resistivity in these systems [26]. As suggested by the HFL theory, the T^2-dependent HFL relaxation rate is taken equally as the Hall scattering rate by $\hbar(\tau_{HFL})^{-1} = T^2/W = \hbar(\tau_H)^{-1}$. According to Anderson's theory [26], the transverse (Hall) scattering rate is determined by scattering between excitations and varies with T^2. The scattering from magnetically active impurities introduces additional terms in the longitudinal transport scattering rate, $1/\tau_{tr}$, and the Hall relaxation rate, $1/\tau_H$. For the transverse scattering rate, Anderson's theory introduced:

$$1/\tau_H = T^2/\hbar J + 1/\tau_M, \tag{2}$$

where J is the spin exchange energy, and $1/\tau_M$ is the impurity contribution. For the Fermi surface formed by spinons, the transport scattering rate of $1/\tau_{tr}$ is proportional to the resistivity, i.e., σ_{xx}, which is proportional to τ_{tr}; whereas, σ_{xy} is proportional to $\tau_H\tau_{tr}$. Thus, the Hall angle $\theta_H = \tan^{-1}(\sigma_{xy}/\sigma_{xx})$ involves $1/\tau_H$ only. Equation (2) implies that:

$$\cot\theta_H = 1/(\omega_c\tau_H) = \alpha T^2 + C, \tag{3}$$

where $\omega_c = eB/m_s$, m_s is the effective transverse mass, and C is the impurity contribution. By combining equations (2) and (3), we can see that α corresponds to $1/(\hbar J\omega_c) \propto B^{-1}$ and $C = 1/(\tau_M\omega_c)$, respectively. From equations (2) and $1/\tau_{HFL} = 1/\tau_H$, as suggested by the HFL theory, we should have $W \approx J$ if the impurity contribution can be neglected. Following Anderson's theory, we write $\theta_H = \omega_c\tau_H = (B/2n\Phi_0)k_F v_k \tau_H$, as described by Chien *et al* [27], where $\Phi_0 = h/2e$ is the flux quantum, $n = k_F^2/2\pi$ is the planar carrier density, k_F is the Fermi wave vector, and $v_k = J/\hbar k_F$. Using equation (3), we now derive a correlation between parameter α and spin exchange energy as:

$$J = (2n\Phi_0/\alpha B)^{1/2} \tag{4}$$

and we have the effective transverse mass, which can be expressed by $m_s = \hbar k_F/v_k = (\hbar k_F)^2/J$. By considering Fermi temperature $T_F = (\hbar k_F)^2/2m_{tr}$, where m_{tr} is the longitudinal transport mass, we find that the ratio of transverse mass to longitudinal mass, β, can be expressed by:

$$\beta \equiv m_s/m_{tr} = 2T_F/J. \tag{5}$$

Equation (5) implies that the transverse mass should be much larger than the longitudinal mass, since $T_F \gg J$ [26, 27]. Apparently, the normal-state Hall measurement provides further insight into the strange-metal transports in superconductors.

In the holographic theory, it is argued that there is only a single contribution from the momentum dissipation to the Hall angle with $\theta_H = (B/Q)\sigma_{diss}$, where Q is the charge density and σ_{diss} is the T^{-2}-dependent dissipation conductivity. Considering that ${\sigma_{diss}}^{-1} = \rho_{e-e} = \Lambda T^2$ with $\Lambda = \frac{\hbar}{e^2}\left(\frac{1}{E_F}\right)^2 \pi A^*$, as previously presented, we obtain $\alpha = Q\Lambda/B = \frac{Q}{B}\frac{\hbar}{e^2}\left(\frac{1}{E_F}\right)^2 \pi A^*$, according to equation (3). Taking $Q = ne$ into account, we can thus denote the measurable parameter α within the holographic theory as

$$\alpha_{holo} = \frac{n}{B}\frac{\hbar}{e}\left(\frac{1}{E_F}\right)^2 \pi A^*. \tag{6}$$

Let us now return to inspect the meaning of parameter α in the HFL theory. According to equation (4), as derived within the framework of the HFL theory, the parameter α can be rewritten as

$$\alpha_{\mathrm{HFL}} = \frac{n}{B}\frac{\hbar}{e}\left(\frac{1}{J}\right)^2 2\pi. \quad (7)$$

Comparing the results shown in equations (6) and (7), one can see that both derived α_{holo} and α_{HFL} exhibit similar formulas, and thus should have the same order of magnitude, since E_{F} and J are the same order of magnitude for strongly correlated systems (see later in the discussion). It is noted that E_{F} is equal to T_{F} when E_{F} is denoted as a temperature unit, and thus, $E_{\mathrm{F}} > J$, as previously mentioned. Both the HFL theory and holographic model propose similar physics, which lie at the origins of the two-lifetime behavior in these so-called 'strange metal' systems. More recently, it has been demonstrated that the separation of transport lifetimes seems to be pervasive in 2D electron liquids [28]. As described in some review articles [10, 29], there are other theoretical approaches that have been proposed for the anomalous transport phenomena in HTS cuprates However, only the mentioned theoretical schemes propose the universal expression of resistivity to describe the crossover of transports from NFL to FL behavior.

To sum up, by measuring longitudinal resistivity $\rho_{xx}(T)$ and Hall angle $\theta_{\mathrm{H}}(T)$, the obtained energy scales W and J are proposed to describe the crossover of transport from NFL-like behavior to FL-like behavior, as well as the electronic correlation strength for these strange-metal systems [18–20]. Although the mechanisms of resistivity are different, both the HFL and holographic theories provide consistent pictures that there exist two transport relaxation times, which independently influence the Hall effect and resistivity in these systems. Based on the schemes within the framework of the HFL and holographic theories, longitudinal resistivity $\rho_{xx}(T)$ and Hall angle $\theta_{\mathrm{H}}(T)$ for BFCA single crystals, as well as some conventional and unconventional superconductors, are examined, as follows.

3. Experiment

Previous works have described the preparations and transport measurements of investigated samples of BFCA single crystals, single-crystal $NaFe_{1-x}Co_xAs$ (NFCA) with $x = 0.022$, and the charge-density-wave (CDW) related superconductors of $Ca_3Ir_4Sn_{13}$ (CaIrSn) and $Sr_3Rh_4Sn_{13}$ (SrRhSn) crystals [30–32]. HTS c-axis oriented $YBa_2Cu_3O_y$ (YBCO) and $NdBa_2Cu_3O_y$ (NBCO) thin films are grown by radio frequency sputtering onto $SrTiO_3$ (001) substrates, as described in literature [33]. $FeSe_{0.5}Te_{0.5}$ (FeSeTe) single crystals have been grown from self-flux in a quartz crucible by referring to the conditions proposed by Sales *et al* [34], exhibiting good crystallization with the c-axis orientation perpendicular to the plane of the crystal slabs. In addition, a piece of Nb metal with purity of 99.9%, which is regarded as a conventional superconductor, has been studied for comparison. Within the transport measurements, a Hall-measurement geometry with five leads is constructed to allow simultaneous measurements of both longitudinal (ρ_{xx}) and transverse (Hall) resistivities (ρ_{xy}) using standard dc techniques.

4. Results and discussion

Figure 1(a) shows the temperature dependence of resistivity for BFCA single crystals with doping levels of $x = 0$, 0.05, 0.08, 0.10, and 0.20. The inset of figure 1(a) shows the low-temperature resistivity for the corresponding samples. As shown, the values of resistivity, transition temperatures, and temperature-dependent behaviors are similar to those reported in [35]. In addition, the undoped parent sample shows a very sharp drop in resistivity at the antiferromagnetic transition temperature of 135 K, which accompanies an additional knee-like transition at 25 K, as seen in the inset of figure 1(a). The additional transition at low temperature is similar to that observed by Rotundu *et al* [36], and seems to be dependent on the annealing periods, which is a phenomenon that has never been examined, and thus, has room for further investigation.

Figure 1(b) shows that the resistivities of the over-doped BFCA with $x = 0.2$ follow the form of $\rho_{xx} = \rho_0 + \Lambda T^2$ with fields of 0 and 6 T at whole temperatures. Here, the applied field is parallel to the current I in order to eliminate the Lorentz contribution from resistivities. The inset of figure 1(b) shows the field dependences of the Λ value and residual resistivity ρ_0. As seen, both Λ and ρ_0 are almost field-independent, and the resistivities in fields reveal tiny magnetoresistance. Indeed, the T^2 dependence of ρ_{xx} and the weak field independence of Λ demonstrate FL-like characteristics in the high-doping BFCA.

Using equation (1), this study attempts to analyze the normal-state BFCA resistivity, as shown in figure 1(a). Equation (1) is fitted to data through the least squares regression method in order to precisely determine parameters A, W, and ρ_0. In addition, figure 1(a) shows the fitting results (solid lines) for BFCA with different doping levels. Figures 2(a) and (b) show the values of the parameters in equation (1), as obtained from the fit as a function of Co doping x. As shown in figure 2(a), the x dependency of energy scale (in temperature unit) W reveals a rapid increase in the over-doping region, which is similar to that observed on $La_{2-x}Sr_xCuO_4$ [18]. The values of W for BFCA, which are in the range of 87–1493 K, are approximately the same order of magnitude as those for $La_{2-x}Sr_xCuO_4$ and other HTS cuprates [19]. Figure 2(b) illustrates the x dependences of parameters A

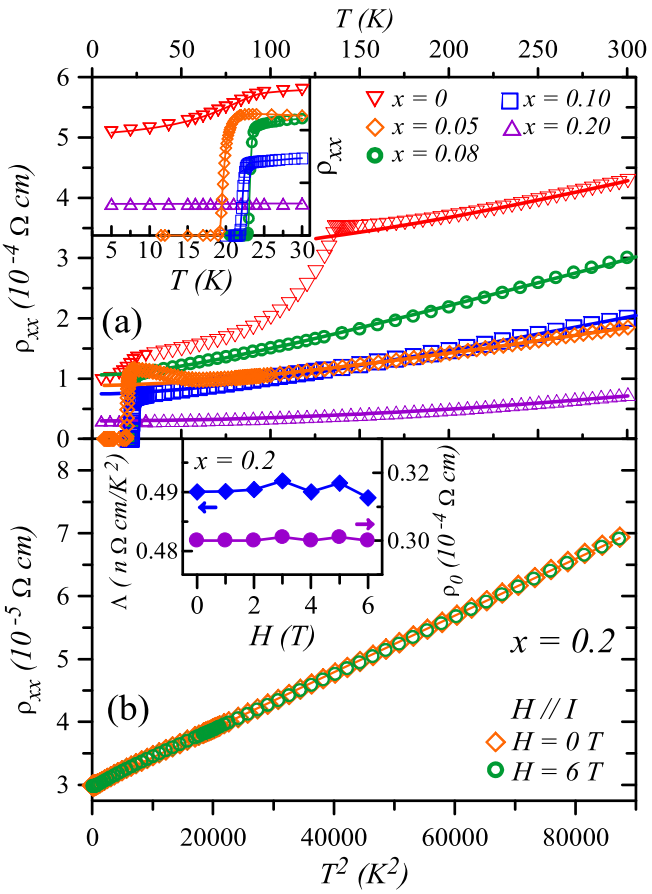

Figure 1. (a) Temperature dependence of resistivity for BFCA single crystals with doping levels of $x = 0, 0.05, 0.08, 0.10$, and 0.20. The solid lines represent the results deduced from the fit of equation (1). (b) Resistivities of the over-doped BFCA with $x = 0.2$ follow the form $\rho_{xx} = \rho_0 + \Lambda T^2$ with fields of 0 and 6 T parallel to the current I (the solid line). The inset shows the field dependences of the Λ value and the residual resistivity ρ_0.

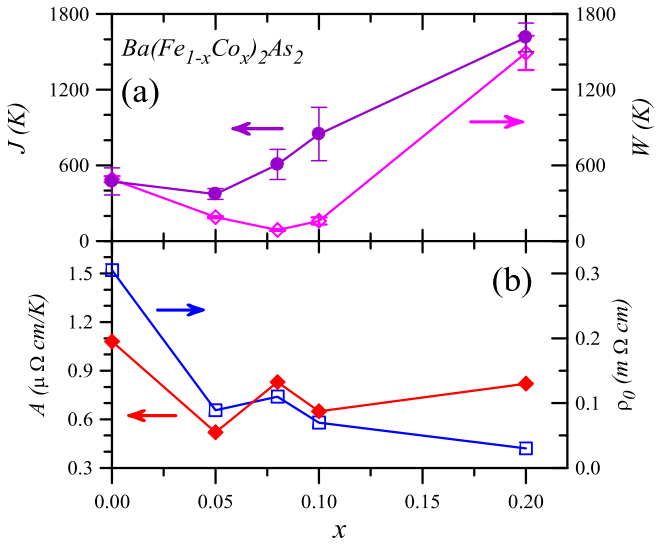

Figure 2. Values of parameters (a) W and (b) A and ρ_0 obtained from the fit of equation (1) as a function of Co doping. In addition, (a) shows the x-dependent spin exchange energy J estimated with equation (4).

and ρ_0. In substance, the values of parameters A and ρ_0 decrease with an increase in x, which is also a behavior similar to that obtained for $La_{2-x}Sr_xCuO_4$. Closer examination of equation (1) shows that, the rapid increase in W for the higher-doping BFCA indeed agrees with the T^2-like resistivity commonly observed both in HTS cuprates and iron-based superconductors, as previously mentioned.

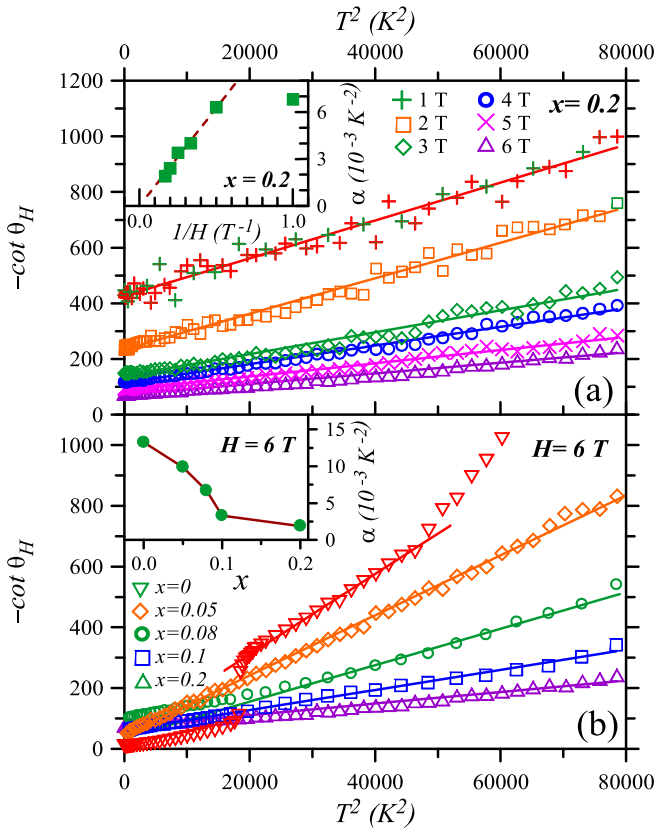

Figure 3. (a) Plots of $-\cot\theta_H$ versus T^2 for BFCA with $x = 0.20$ in various applied fields up to 6 T. The solid lines denote the results of the fit to equation (3). (b) Plots of $-\cot_H$ versus T^2 for BFCA with different doping levels measured in the field of 6 T. The solid lines represent the fit of equation (3) in the normal-state temperature region. The inset of (a) shows the parameter α against H^{-1}. The dashed line shows that $\alpha \propto H^{-1}$ at fields larger than 2 T. The inset of (b) shows the x dependence of parameter α obtained in the field of 6 T.

Figure 3(a) plots $-\cot\theta_H$, as defined by $\cot\theta_H = \rho_{xx}/\rho_{xy}$, versus T^2 for BFCA with $x = 0.20$ in various applied fields up to 6 T. As can be seen, the data fall almost in a straight line in the studied temperature range, and can be fitted to equation (3). The inset of figure 3(a) shows parameter α against H^{-1}, and demonstrates that α is indeed proportional to H^{-1} at fields larger than 2 T, which is consistent with the predicted previously result. The deviation of $\alpha \propto H^{-1}$ at low fields implies the occurrence of field-dependent parameters J or m_s at low fields; however, this phenomenon remains to be further debated.

Figure 3(b) plots $-\cot\theta_H$ versus T^2 for BFCA with different doping levels measured in the field of 6 T. As can be seen, the data also fall in a straight line in the normal-state temperature region, and can be fitted to equation (3). The inset of figure 3(b) shows the x dependence of parameter α obtained in the field of 6 T. The values of α for BFCA decrease with an increase in x, and are approximately the same order of magnitude as those for HTS cuprates [27]. Furthermore, with equation (4), we can estimate the values of J for BFCA samples, as shown in figure 2(a), where the planar carrier density is calculated by $n = (3\pi^2 n_{3D})^{2/3}/2\pi$ and the volume carrier density n_{3D} is obtained from the Hall measurement. From figure 2(a), we note that, the error bar of the J value rises from the n_{3D} values taken at different temperature regions. It is found that the values of J are almost the same as the W values for BFCA with $x = 0$ and 0.20; and while the J values are larger than those of W, they are of the same order of several hundred Kelvin for BFCA with $x = 0.10$, which is in agreement with the HFL theory. This result indicates that the transports in over-doped BFCA and in their parent compound ($x = 0$) can be described by the HFL scenario.

Next, this study attempts to extend this observation into a new phase diagram for BFCA. According to the HFL or holographic resistivity in equation (1), one can see that the resistivity behaves as $\rho_{xx} \propto T$ or $\rho_{xx} \propto T^2$, and according to whether $T \gg W$ or $T \ll W$. First consider the attempt to draw a line up and to the right from QCP (i.e. the optimum-doped point) and the result of $W \approx 3.5T_c$ ($W \approx 87.4$ K, and $T_c \approx 25$ K) for the optimum-doped BFCA with $x = 0.08$, which should behave like a NFL character at temperatures above T_c. We thus draw a line of $W/3.5$ for BFCA in the higher-doping region up and to the right from QCP in order to show the crossover from NFL-like behavior to FL-like behavior at high doping, as seen in figure 4. In addition, surprisingly, the $W/3.5$ line almost merges into the boundary line of the antiferromagnetic (AFM) transition for the under-doped

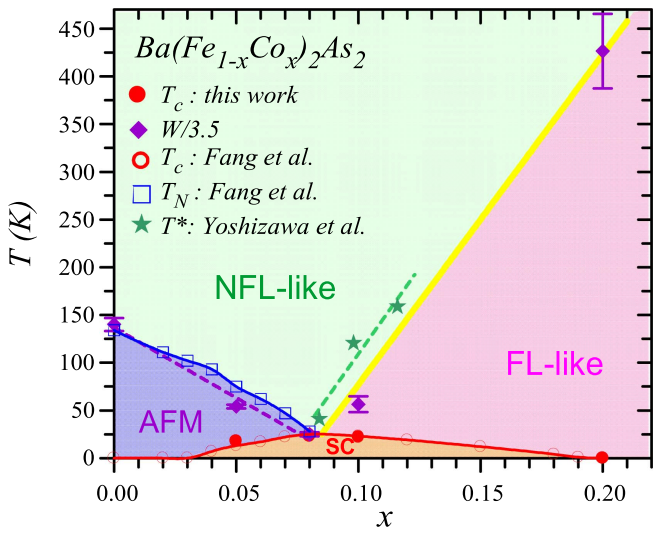

Figure 4. Renewed phase diagram for BFCA, as extracted from this work and previous reports, for comparison. A line of $W/3.5$ for BFCA, as drawn in the higher-doping region up and to the right from QCP, shows the crossover from NFL-like behavior to FL-like behavior. Some data are extracted from previous reports for comparison.

BFCA. Figure 4 also illustrates the phase-transition diagram extracted from previous reports [23, 35] for comparison, and reveals a renewed phase diagram for BFCA.

Yoshizawa *et al* [37] recently investigated the elastic properties of BFCA single crystals with different Co concentrations, in which elastic constant C_{66} shows large elastic softening associated with the structural phase transition. They obtained characteristic temperature T^* with the deviation of the inverse of C_{66} from the T-linear behavior, and inferred that T^* possibly corresponds to the crossover from the NFL region to the FL region. Figure 4 also illustrates the duplicated T^* values for comparison, and shows an approximate coincidence between the $W/3.5$ boundary line and T^* values. In addition, the derived values of bandwidth W, by Yoshizawa *et al* present the same order of several hundred Kelvin for higher-doped BFCA as those obtained herein with the HFL and holographic transport theories. Furthermore, the factor of 3.5 indicates that the crossover temperature corresponds to a fractional value of bandwidth.

Further discussion of the exchange energy J in superconductors via equations (4) and (5) suggests that the exchange energy can seemingly manipulate the transport behaviors in superconductors. An interesting issue is to examine the spin exchange energy in different kinds of superconductors in order to debate their electronic correlation. Figure 5(a) illustrates the basic characteristics of resistive transition for some high-quality superconductors, including the optimum-doped BFCA, NFCA, and FeSeTe crystals, fully oxygenized YBCO and NBCO films, and the CDW-related superconducting CaIrSn and SrRhSn crystals, as described in the Experiment section, and a conventional superconductor of Nb metal. As seen, the measured superconducting transition temperatures are almost the same as those previously reported.

Figure 5(b) plots $|\cot\theta_H|$ versus T^2 for the corresponding samples measured in the field of 6 T. As can be seen, the data also fall in a straight line in the normal-state temperature region, and can be fitted to equation (3). As mentioned above, the exchange energy offers the key to understanding the electric correlation in superconductivity. Following the analysis previously conducted in BFCA, we can derive the exchange energy according to the data in figure 5(b) by using equation (4). The inset of figure 5(b) shows J versus T_c for the corresponding samples in figure 5(b); however, there is no clear relation between J and T_c. Recently, it has been pointed out that, the ratio of T_c to Fermi temperature T_F characterizes the correlation strength in superconductors [38]. In unconventional superconductors, such as iron-based superconducting $FeTe_{0.6}Se_{0.4}$, HTS YBCO, and heavy fermion superconductors, this ratio is about 0.1; however, it is only ~0.02 in conventional BCS superconductors [38]. Being analogous to the analysis of T_c/T_F, we are motivated to examine the ratio of J/T_F in different kinds of superconductors.

Figure 6(a) shows T_c as a function of Fermi temperature T_F for the superconductors studied herein. The Fermi temperature T_F can be extracted from [39]:

$$S/T = \pm \frac{\pi^2}{2}\frac{k_B}{e}\frac{1}{T_F} \text{ or}$$

$$\gamma = \frac{\pi^2}{3}k_B\frac{n_{3D}}{T_F},$$

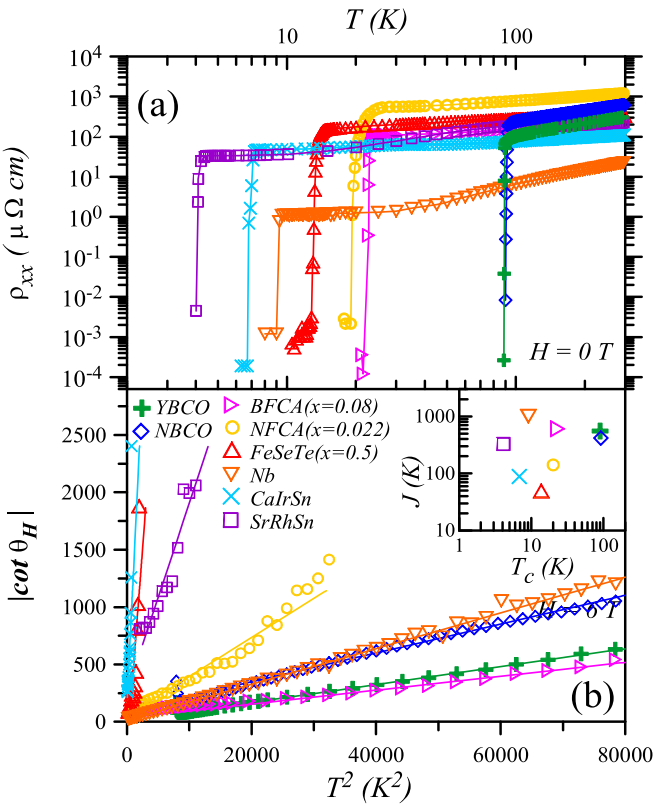

Figure 5. (a) Basic characteristics of resistive transition for some high-quality superconductors as mentioned in the text. (b) Plots of $|\cot\theta_H|$ versus T^2 for the corresponding samples measured in the field of 6 T. The solid lines represent the fit of equation (3) in the normal-state temperature region. The inset of (b) shows J versus T_c for the corresponding samples.

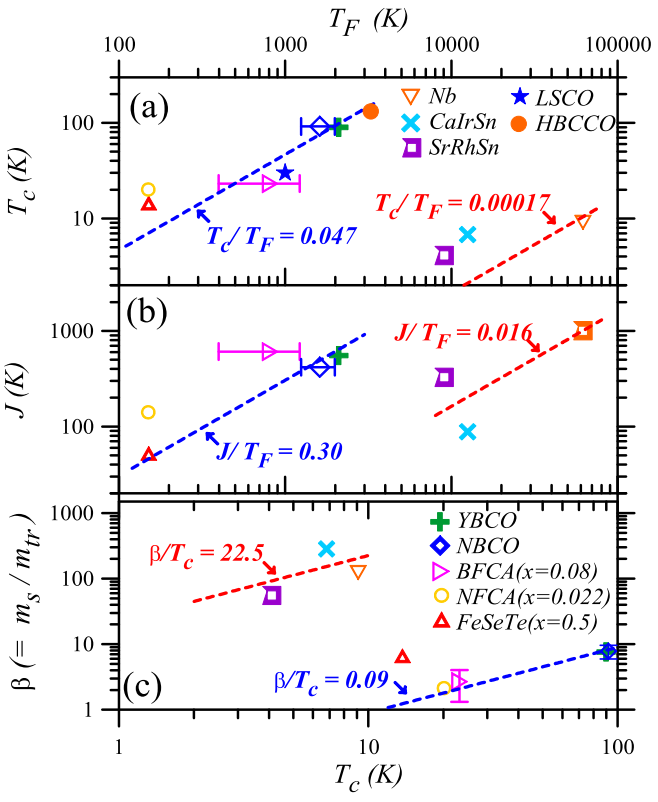

Figure 6. (a) T_c and (b) J versus Fermi temperature T_F for the superconductors studied. (c) β, as expressed in equation (5), as a function of T_c for the superconductors studied. The dashed lines represent the parameter ratios for strongly correlated and weakly correlated superconductors as indicated.

where S is the Seebeck coefficient, γ is a T-linear electronic specific heat coefficient, k_B is Boltzmann's constant, and e is the electron charge. This study adopts the results of thermal transport for NBCO [40, 41], BFCA [42, 43], NFCA [44], SrRhSn [45], and Nb [46] to make the estimations of T_F, while the T_F values of YBCO, FeSeTe, and CaIrSn are duplicated from articles in literature [38, 47, 48].

However, as shown in figure 6(a), the error bars of T_F arise from the various n_{3D} values, as taken at normal-state temperatures, and some divergences in the values of S and γ reported. The data for $HgBa_2Ca_2Cu_3O_{8+\delta}$ (HBCCO) and $La_{1.85}Sr_{0.15}CuO_4$ (LSCO) are adopted from [48] for comparison. Figure 6(a) shows the dash lines of $T_c/T_F = 0.047$ and 0.000 17 for two groups of superconductors, respectively. The data of the first group of superconductors, including the strongly correlated HTS YBCO and NBCO, and iron-based superconducting BFCA, NFCA, and FeSeTe, follow the line of $T_c/T_F = 0.047$, while the data of the second group of superconductors, including weakly correlated CaIrSn, SrRhSn, and Nb, are distributed over the region near the line of $T_c/T_F = 0.000\ 17$. This result is in accordance with previously reported results [38, 47, 48].

Inspired by the plot in figure 6(a), in figure 6(b) we demonstrate a plot to point out an intimate link between J and T_F in a superconducting system. An interesting result is that the data of the strongly correlated superconductors (first group) follow the line of $J/T_F = 0.30$, while the data of the weakly correlated superconductors (second group) follow the line of $J/T_F = 0.016$. This finding indicates that the ratio of J to the Fermi temperature T_F can also characterize the correlation strength in superconductors. It is inferred that, for a strongly correlated superconductor, this ratio is much larger than that for a conventional BCS superconductor due to their smaller T_F values.

This study further examines the ratio of transverse mass to longitudinal mass, β, as expressed in equation (5). Figure 6(c) illustrates β as a function of T_c for the superconductors studied herein, which shows that the strongly correlated superconductors reveal smaller β values, while larger β values are obtained for the weakly correlated superconductors. The β values for the strongly correlated superconductors approximately follow the line of $\beta/T_c = 0.09$, while the data of the weakly correlated superconductors follow the line of $\beta/T_c = 22.5$, indicating that the ratio of β to T_c also correlates closely with the electronic correlation strength in superconductors. This result implies that there are different effects of electronic correlation on the ratio of transverse mass to longitudinal mass between strongly and weakly correlated superconductors. Generally speaking, it can be understood that, even though T_c is enhanced, such as in the strongly correlated superconductors, the longitudinal effective mass increases faster than the transverse effective mass, leading to a smaller β value due to the relatively small value of T_F. We can see that the correlation strength in superconductors can be experimentally revealed by the normal-state Hall angle, thus, more theoretical or experimental studies on the effects of electronic correlation in superconductors are necessary.

Having observed that correlation strength can be characterized by these derived parameters, one may further proceed to the debate between the HFL theory and holographic theory on the basis of the experimental data. According to the derivations in the previous section, it is worthy to notice that the value of Fermi energy E_F, which is a key parameter related to the electronic state, can be respectively derived from the experimental data of pre-factor A (corresponds to the coefficient in T-linear resistivity as $T \gg W$) and parameter α, as based on the HFL and holographic theories. The obtained E_F from pre-factor A, as based on the HFL and holographic theories, are denoted by $E_{F,HFL}$ and $E_{F,holo}$, respectively, and can be expressed by $E_{F,HFL} = \frac{\hbar}{e^2}\frac{1}{A}\left(\frac{v_{F0}}{v_F}\right)$ and $E_{F,holo} = \frac{\hbar}{e^2}\frac{1}{A}4\pi^2\lambda$. Moreover, the value of E_F can also be obtained from parameter α, as based on the holographic theory seen in equation (6), which is denoted by $E_{F,holo,\alpha}$, to have $E_{F,holo,\alpha} = \left(\frac{n}{B}\frac{\hbar}{e}\frac{1}{\alpha}\pi A^*\right)^{1/2}$.

Table 1 illustrates the obtained parameters of T_c, A, α, $E_{F,HFL}$, $E_{F,holo}$, $E_{F,holo,\alpha}$, T_F, and J for the BFCA samples. In addition, the parameters of HTS YBCO and NBCO films are shown for discussion. Here, the parameters of T_c, A, α, T_F, and J are obtained from the experimental results or calculations, as previously mentioned, where the A values for YBCO and NBCO films are obtained by their well linear fit to their $\rho(T)$ data from 120–300 K. Again notice that the large error bars of T_F arise from the various n_{3D} values, as taken at normal-state temperatures, and some divergences in the values of S and γ reported. In addition, we replace the A values of bulk resistivity with the A/t values for calculation of the 2D sheet resistance, as described by theories, where t is taken as the c-axis length of the unit cell with $t \approx 1.3$ and 1.2 nm for BFCA and HTS cuprates, respectively. Regarding calculation of the values of $E_{F,HFL}$, $E_{F,holo}$, and $E_{F,holo,\alpha}$, the information of (v_{F0}/v_F), λ, and A^* for BFCA and HTS cuprates should be clarified. Considering the small anisotropic transport properties of BFCA and HTS cuprates in the crystal ab plane, we take $(v_{F0}/v_F) \approx 1$, as shown in [18]. The values of λ for BFCA and HTS cuprates are taken as 0.12 and 0.3, respectively, by referring to the results in [49, 25]. The A^* value of ~4 for BFCA is estimated by Rullier-Albenque *et al* [1], while the A^* value for the HTS cuprates has not been reported yet. As previously mentioned, A^*describes the electron–electron scattering processes given by $\hbar/\tau_{e-e} = A^*T^2/E_F$, thus, A^* can be estimated from the Λ coefficient of T^2-dependent resistivity, that $\rho = m_{tr}/ne^2\tau_{e-e} = (m_{tr}/ne^2)A^*T^2/(\hbar E_F) = \Lambda T^2$. It has been reported that the Λ value of YBCO is $\sim 1.5 \times 10^{-9}\ \Omega\ \text{cm K}^{-2}$ and the Hall coefficient is $R_H = 1/ne \approx 5 \times 10^{-4}\ \text{cm}^3\ \text{C}^{-1}$ [50].

Table 1. Obtained parameters of T_c, A, α, $E_{F,HFL}$, $E_{F,holo}$, $E_{F,holo,\alpha}$, T_F, and J for BFCA samples, YBCO, and NBCO films. The T_F of YBCO is taken from [38].

Samples BFCA	T_c K	A $\mu\Omega$ cm K^{-1}	α (6 T) 10^{-3} K^{-2}	$E_{F,HFL}$ K	$E_{F,holo}$ K	$E_{F,holo,\alpha}$ K	T_F K	J K
$x = 0$	—	1.08 ± 0.01	13.3 ± 0.3	495 ± 5	2345 ± 24	669 ± 153	682 ± 305	473 ± 108
$x = 0.05$	19.1	0.52 ± 0.01	9.91 ± 0.05	1027 ± 20	4858 ± 95	527 ± 61	778 ± 283	373 ± 43
$x = 0.08$	22.9	0.83 ± 0.02	6.70 ± 0.03	643 ± 161	3048 ± 76	858 ± 170	811 ± 413	607 ± 120
$x = 0.10$	21.8	0.65 ± 0.02	3.31 ± 0.03	822 ± 25	3894 ± 120	1199 ± 300	1009 ± 197	848 ± 212
$x = 0.20$	—	0.82 ± 0.01	1.90 ± 0.03	651 ± 8	3084 ± 36	2285 ± 161	1000 ± 204	1616 ± 114
YBCO	89.8	1.02 ± 0.01	7.80 ± 0.06	483 ± 5	5719 ± 59	1042 ± 4	2100	553 ± 2
NBCO	91.8	1.82 ± 0.01	12.5 ± 0.1	271 ± 2	3209 ± 24	784 ± 4	1616 ± 371	416 ± 2

By considering $E_F = 2100$ K [38] and $m_{tr} \approx 12m_e$ [51], we obtain an A^* value of ~7.1 for YBCO, and then, proceed to calculate the $E_{F,holo,\alpha}$ values of YBCO and NBCO.

As seen in table 1, the obtained $E_{F,HFL}$ values for BFCA, which are in the range of 495–1027 K, are near the T_F values of 682 ± 305–1009 ± 197 K, which are derived according to the reported electronic specific heat coefficients [43]. However, the obtained $E_{F,HFL}$ values for YBCO and NBCO are much smaller than those of T_F, implying that the assumption of $(v_{F0}/v_F) \approx 1$ may need to be corrected when applying the HFL theory to HTS cuprates. On the other hand, all $E_{F,holo}$ values for BFCA, YBCO, and NBCO are almost several-time magnitude larger than those of T_F, while $E_{F,holo,\alpha}$ shows a more consistent result, as compared with the values of T_F. These deviations may arise from the uncertain parameters of λ and A^* for iron-based superconductors and HTS cuprates, which require further confirmation through experimentation. If any doubt remains about these derived E_F values, it is clear that both the HFL and holographic theories hold truths regarding the temperature-dependent resistivity and Hall angle in these strange-metal superconductors, and some uncertain parameters still require further calibration for theoretical application.

5. Conclusions

By considering HFL and holographic theories, this research examined spin exchange energy J and model-dependent energy scale W in BFCA single crystals, as deduced from the Hall angles and resistivities, respectively. In theoretical surveys, both HFL and holographic theories give similar physics, meaning that there exist two transport relaxation times, which independently influence the Hall effect and resistivity in the so-called 'strange metal' systems. One can see that the values of J are almost the same as the W values, or are of the same order of several hundred Kelvin for the over-doped BFCA, which is in agreement with the HFL theory. Moreover, a drawn line of $W/3.5$ for BFCA in the higher-doping region up to the right from QCP shows the crossover from NFL-like behavior to FL-like behavior at high doping, leading to the obtainment of a new phase diagram for BFCA. Furthermore, this study has newly derived spin exchange energies and Fermi temperatures for some conventional and unconventional superconductors from Hall measurements in order to explore their electronic correlation strength. Findings show that the data of T_c/T_F and J/T_F for strongly correlated superconductors follow higher-ratio lines, as compared with those for weakly correlated superconductors. By contrast, the ratios of transverse mass to longitudinal mass for strongly correlated superconductors reveal smaller values. The ratios of T_c/T_F, J/T_F, and β/T_c are presented, for the first time, as characterizing the correlation strength in superconductors. In addition, both the HFL and holographic theories can describe the temperature-dependent resistivity and Hall angle in these unconventional superconductors, which have some uncertain parameters that require further experimental confirmation.

Acknowledgments

The authors thank the Ministry of Science and Technology of Taiwan for financial support under Grant Nos. 104-2112-M-002-008-MY2 (LMW), MOST-103-2112-M-006-014-MY3, and MOST-103-2119-M-006-014-MY3 (CSL).

References

[1] Rullier-Albenque F, Colson D, Forget A and Alloul H 2009 *Phys. Rev. Lett.* **103** 057001
[2] Lee S, Choi K-Y, Jung E, Roh S, Shin S, Park T and Hwang J 2015 *Sci. Rep.* **5** 12156
[3] Laliberté F *et al* 2011 *Nat. Commun.* **2** 432

[4] Kasahara S et al 2010 Phys. Rev. B 81 184519
[5] Chowdhury D, Orenstein J, Sachdev S and Senthil T 2015 Phys. Rev. B 92 081113
[6] Wang X F, Wu T, Wu G, Liu R H, Chen H, Xie Y L and Chen X H 2009 New J. Phys. 11 045003
[7] Gong D, Xie T, Lu X, Ren C, Shan L, Zhang R, Dai P, Yang Y, Luo H and Li S 2016 Phys. Rev. B 93 134520
[8] Doiron-Leyraud N and Taillefer L 2012 Physica C 481 161
[9] Jin K, Butch N P, Kirshenbaum K, Paglione J and Greene R L 2011 Nature 476 73
[10] Naira S, Wirtha S, Friedemanna S, Steglicha F, Sic Q and Schofield A J 2012 Adv. Phys. 61 583
[11] Cooper R A et al 2009 Science 323 603
[12] Bucher B, Steiner P, Karpinski J, Kaldis E and Wachter P 1993 Phys. Rev. Lett. 70 2012
[13] Dai Y M, Xu B, Shen B, Xiao H, Wen H H, Qiu X G, Homes C C and Lobo R P S M 2013 Phys. Rev. Lett. 111 117001
[14] Chubukov A V, Maslov D L and Yudson V I 2014 Phys. Rev. B 89 155126
[15] Moon S J et al 2014 Phys. Rev. B 90 014503
[16] Tanatar M A et al 2014 Phys. Rev. B 89 144514
[17] Matusiak1 M and Wolf T 2015 Phys. Rev. B 92 020507
[18] Anderson P W and Casey P A 2009 Phys. Rev. B 80 094508
[19] Casey P A and Anderson P W 2011 Phys. Rev. Lett. 106 097002
[20] Blake M and Donos A 2015 Phys. Rev. Lett. 114 021601
[21] Xu W, Haule K and Kotliar G 2013 Phys. Rev. Lett. 111 036401
[22] Zhou R, Li Z, Yang J, Sun D L, Lin C T and Zheng G 2013 Nat. Commun. 4 2265
[23] Doiron-Leyraud N, Auban-Senzier P, René de Cotret S, Bourbonnais C, Jérome D, Bechgaard K and Taillefer L 2009 Phys. Rev. B 80 214531
[24] Castro H and Deutscher G 2004 Phys. Rev. B 70 174511
[25] Ito T, Takenaka K and Uchida S 1993 Phys. Rev. Lett. 70 3995
[26] Anderson P W 1991 Phys. Rev. Lett. 67 2092
[27] Chien T R, Wang Z Z and Ong N P 1991 Phys. Rev. Lett. 67 2088
[28] Mikheev E, Freeze C R, Isaac B J, Cain T A and Stemmer S 2015 Phys. Rev. B 8691 165125
[29] Kontani H 2008 Rep. Prog. Phys. 71 026501
[30] Wang L M, Sou U C, Yang H C, Chang L J, Cheng C M, Tsuei K D, Su Y, Wolf T and Adelmann P 2011 Phys. Rev. B 83 134506
[31] Wang L M, Wang C Y, Sou U C, Yang H C, Chang L J, Redding C, Song Y, Dai P and Zhang C 2013 J. Phys.: Condens. Matter 25 395702
[32] Wang L M, Wang C Y, Chen G M, Kuo C N and Lue C S 2015 New J. Phys. 17 033005
[33] Yang H C, Wang L M and Horng H E 1997 Physica C 281 325
[34] Sales B C, Sefat A S, McGuire M A, Jin R Y, Mandrus D and Mozharivskyj Y 2009 Phys. Rev. B 79 094521
[35] Fang L et al 2009 Phys. Rev. B 80 140508
[36] Rotundu C R et al 2010 Phys. Rev. B 82 144525
[37] Yoshizawa M et al 2012 J. Phys. Soc. Japan 81 024604
[38] Pourret A, Malone L, Antunes A B, Yadav C S, Paulose P L, Fauqu´e B and Behnia K 2011 Phys. Rev. B 83 020504(R)
[39] Behnia K, Jaccard D and Flouquet J 2004 J. Phys.: Condens. Matter 16 5187
[40] Neeleshwar S, Muralidhar M, Murakami M and Reddy P V 2003 Physica C 391 131
[41] Tutsch U, Schweiss P, Wühl H, Obst B and Wolf T 2004 Eur. Phys. J. B 41 471
[42] Hardy F, Adelmann P, Wolf T, Löhneysen H V and Meingast C 2009 Phys. Rev. Lett. 102 187004
[43] Hardy F, Burger P, Wolf T, Fisher R A, Schweiss P, Adelmann P, Heid R, Fromknecht R, Eder R and Ernst D 2010 Europhys. Lett. 91 47008
[44] Wang A F, Luo X G, Yan Y J, Ying J J, Xiang Z J, Ye G J, Cheng P, Li Z Y, Hu W J and Chen X H 2012 Phys. Rev. B 85 224521
[45] Kase N, Hayamizu H and Akimitsu J 2011 Phys. Rev. B 83 184509
[46] Ashcroft N W and Mermin N D 1976 Solid State Physics (Philadelphia, PA: Saunders)
[47] Wang K and Petrovic C 2012 Phys. Rev. B 86 024522
[48] Sarrao J L and Thompson J D 2007 J. Phys. Soc. Japan 76 051013
[49] Mansart B, Boschetto D, Savoia A, Rullier-Albenque F, Bouquet F, Papalazarou E, Forget A, Colson D, Rousse A and Marsi M 2010 Phys. Rev. B 82 024513
[50] Stojković B P and Pines D 1996 Phys. Rev. Lett. 76 811
[51] Harshman D R and Mills A P Jr 1992 Phys. Rev. B 45 10684